Analyst

Single Cell Analysis of Aged RBCs: Quantitative analysis of the aged cells and byproducts.

Journal:	*Analyst*
Manuscript ID	AN-ART-10-2018-001904.R1
Article Type:	Paper
Date Submitted by the Author:	30-Nov-2018

Complete List of Authors:	Kim, James; Ohio State University William G Lowrie Department of Chemical and Biomolecular Engineering Weigand, Mitchell; Ohio State University William G Lowrie Department of Chemical and Biomolecular Engineering Palmer, Andre; Ohio State University Columbus, Department of Chemical and Biomedical Engineering Zborowski, Maciej; Lerner Research Institute, Department of Biomedical Engineering Yazer, Mark; University of Pittsburg, Pathology Chalmers, Jeffrey; The Ohio State University, William G. Lowrie Department of Chemical and Biomolecular Engineering

Analyst: Submission

ARTICLE

Single Cell Analysis of Aged RBCs: Quantitative analysis of the aged cells and byproducts.

Kim, James, [a] Weigand, Mitchell,[a] Palmer, Andre F.,[a] Zborowski, M.,[b] Yazer, M.H. ,[c]

Chalmers, Jeffrey J.[a,†]

www.rsc.org/

This study initially focused on characterizing the aging process of red blood cells by correlating the loss of hemoglobin and the translocation of the phosphatidylserine (PS) in expired human red blood cells, hRBCs. Five pre-storage, leukoreduced hRBC units in AS-5 solution were stored between 1 - 6 ºC for 42 days. Aliquots from each of these units were stained with Annexin-V FLUOS, which binds to externalized PS, and the hemoglobin within the cells were placed in a methehemoglobin state with sodium nitrite, metHb. These aliquots were subsequently sorted into four sub-populations, ranging from no PS expression to high PS expression using a BD FACS ARIAIII. Each of these sub-fractions were introduced into the Cell Tracking Velocimetry apparatus which measured both the magnetically and gravity induced velocity. Subsequently, the samples were removed from the Cell Tracking Velocimetry instrument and characterized using the Multisizer 4e Coulter Counter. From the magnetic induced velocity, the amount of hemoglobin, in pg Hb/cell can be determined, and using an average value of the density of RBCs, the size can be determined. For PS negative sub-fraction of RBCs, the size of the RBC was as expected but the average hemoglobin, Hb, content was below the threshold which defines anemia. In contrast, unexpected results were observed with the various levels of expression of PS. First, virtually all of the PS expressing cells were significantly smaller, on the order of 1 micron, than a normal RBC after 42 days of storage; yet the density of these small cells/microvessicles, had density such that they had settling velocities similar to normal sized RBCs. Further, while the total amount of Hb per small cell/microvessicle, was only approximately 25% of the full-sized RBCs, the volume of these small cell/microvessicle is only 1/200 of the PS negative RBCs. This suggests that these PS expressing cells are shrunken RBCs, or shrunken microvessicles from RBCs that concentrated the Hb internally. These results suggest not only a relationship between the loss of hemoglobin, and the amount of PS exposed on the cellular outer wall, but also a mechanism by which these aged RBCs break down. It is not known at this time if this is an artifact of storage, or similar mechanism occur in circulation within the human body.

Introduction

The most recent statistics from the 2015 National Blood Collection and Utilization Survey reported the collection of 12.6 million whole blood and red blood cell (RBC) units in the US.[1] However, a decreasing trend in the number of RBCs distributed to hospitals from blood collection centers both in the US and around the world has been recently documented.[2] Although human RBC (hRBC) units can be stored between 1-6 °C for up to 42 days,[3] in 2015 approximately 242,000 units outdated in the blood center, while 426,000 units expired in hospital transfusion services, before use.[1] While 11.3 million RBC units were transfused in 2015, this small surplus of RBCs does not reflect the day-to-day inventory at the local blood collector or hospital transfusion service. These surplus RBCs are not distributed evenly across the country at all times of the year nor are they necessarily of the most common blood groups, thus potentially making it difficult to find suitable recipients for these units.[4] RBC unit shortages can cause major patient morbidity such as forcing the cancelation of elective surgeries when supplies are critically low, which can happen in emergency situations such as during natural or man-made disasters or during holiday periods.[5,6] Hence, there is a need to have a mechanism in place to have enough

[a.] *William G. Lowrie Department of Chemical and Biomolecular Engineering, The Ohio State University,320 Koffolt Laboratories, 151 West Woodruff Avenue, Columbus, OH 43210*
[b.] *Department of Biomedical Engineering, Cleveland Clinic, 9500 Euclid Avenue, Cleveland, OH 44195.*
[c.] *Department of Pathology, University of Pittsburgh and The Institute for Transfusion Medicine, University of Pittsburgh, 3636 Blvd of the Allies, Pittsburgh, PA 15213*
† To whom correspondence should be addressed: Jeffrey J. Chalmers, William G. Lowrie Department of Chemical and Biomolecular Engineering, The Ohio State University, 151 West Woodruff Avenue, Columbus, OH 43210, Email: Chalmers@chbmeng.ohio-state.edu, Tel: (614)292-2727

RBC units of the right blood groups available at all times to minimize schedule disruptions and patient morbidity.

Significant research has been, and is being conducted, on the characterization of RBCs with respect to their aging process while they are being stored in the blood bank awaiting transfusion. As RBCs are stored, they undergo changes, some of which are permanent. This so-called RBC "storage lesion" affects all aspects of the RBC, including the membrane, which undergoes alterations in its biochemistry, loss of cell surface area, and shedding of hemoglobin (Hb)-containing vesicles. In cold storage, progressive aggregability, reduced levels of cell membrane stomatin, increased cell rigidity, and increased translocation of phosphatidylserine (PS) from the intracellular RBC membrane bilayer to the extracellular membrane bilayer where it is exposed to the outside environment. [7] It is known that only ~75% of the RBCs from units with a mean storage age of 30 days survive in a human recipient beyond the first 24 hours following transfusion. Fresher RBC units, at a mean of 5 days of storage, feature >85% recovery at 24 hours.[8] However, in both cases, a large quantity of RBCs are quickly removed from the circulation by the reticuloendothelial system (RES). Several reviews[9–15] have highlighted the possible dangers associated with the transfusion of longer stored RBCs and the targeted delivery of iron to the RES through these senescent RBCs that occurs during RBC transfusion. The main clinical effects of transfusing older RBCs are postulated to include impaired O_2 delivery, high plasma potassium ion levels in the recipient (i.e. hyperkalemia), iron overload, complications due to Hb microparticles (i.e. Hb vesicle) formation, cell-free Hb, and an imbalance in nitric oxide (NO) homeostasis. Iron overload may occur when clearance mechanisms of damaged RBCs (i.e. splenic macrophages or Kupffer cells in the liver[16–18]) and clearance mechanisms of cell-free Hb and Hb degradation products (i.e. haptoglobin, hemopexin, transferrin, heme oxygenase[19–21]) become saturated. This can induce inflammation and iron toxicity in organs involved in RBC and Hb clearance[22,23]. Lastly, transfusion of stored RBCs along with Hb microvesicles and cell-free Hb derived from the stored unit along with *in vivo* intravascular hemolysis that occurs after RBC transfusion can induce an imbalance in NO homeostasis, triggering vasoconstriction and hypertension[24–26]. Thus, removing the senescent RBCs from units that are about to be transfused could potentially improve the quality of the RBC unit and reduce the risk of adverse events for the recipients of these units.

In 1936, Pauling and Coryell observed that deoxygenated Hb (deoxyHb) and oxidized Hb (metHb) both have a paramagnetic moment due to unpaired electrons on the heme iron, while oxygenated Hb (oxyHb) has a diamagnetic moment.[27,28] Over the last 20 years, the Chalmers and Zborowski laboratory have developed an instrument which can characterize this magnetic characteristic of RBCs, the instrument is referred to as Cell Tracking Velocimetry (CTV), or single cell magnetophoresis.[29–33]

The CTV instrument tracks the magnetically induced motion of individual cells (or particles) in a glass channel; from which the magnetically and gravity induced velocity are determined. These two velocities are mathematically defined as:

$$u_m = \frac{(\chi_{Cell} - \chi_{Fluid})V_{Cell}}{3\pi D_{Cell}\eta} S_m \quad (1)$$

$$u_s = \frac{(\rho_{Cell} - \rho_{Fluid})V_{Cell}}{3\pi D_{Cell}\eta} g \quad (2)$$

Where $\boldsymbol{\chi}_{cell}$ and $\boldsymbol{\chi}_f$ is the volume magnetic susceptibility of the cell and the buffer, ρ_{cell}, ρ_f is the density of the cell and fluid, V_{cell} and D_{cell} is the volume and equivalent spherical diameter of a cell (particle), η is the viscosity of the suspending fluid and g is the standard gravitational acceleration (9.8 m/s^2). S_m, the magnitude of magnetic energy density gradient, is defined by:

$$S_m = \frac{|\nabla B^2|}{2\mu_0} \quad (3)$$

where μ_0 and B are the permeability of free space and flux density of the source. The CTV instrument is capable of tracking hundreds to thousands of particles.

In the case of RBCs, the magnetic susceptibility (volumetric susceptibility, SI unit system), and correspondingly, the concentration of Hb (mol/L) in each cell can be determined:

$$\chi_{RBC} = \left(\frac{u_m}{u_s}\right)(\Delta\rho)\left(\frac{g}{S_m}\right) + \chi_{H_2O} \quad (4)$$

$$c_{Hb} = \frac{(\chi_{RBC} - \chi_{H_2O})}{(\chi_{m,\,metHb} + \chi_{m,\,globin} - \chi_{H_2O}) \cdot V_{m,\,Hb}} \left[{}^{mol}/_{L}\right] \quad (5)$$

$$mass\ of \frac{Hb}{cell}\left(\frac{pg\ Hb}{cell}\right) = c_{Hb}(GMW\ of\ Hb) \cdot V_{cell} \quad (6)$$

where $V_{m,Hb}$ = 48.23 L/mol is the molar volume of metHb, $\chi_{m,globin}$ = -37,830 $\times$ 10^{-9} L/mol is the molar susceptibility of the globin chain, and χ_{H2O} = -12.97 $\times$ 10^{-9} L/mol is the molar susceptibility of water. The molar susceptibility of the deoxyHb heme group is $\chi_{m,deoxyHb}$ = 50,890

$\times 10^{-9}$ L/mol, and that of metHb heme group is $\chi_{m,metHb}$ = 56,000 $\times$ 10^{-9} L/mol (all in CGS system of units). Using the CTV instrument and these relationships, Chalmers et al. (2017) demonstrated that RBCs, stored in a FDA approved storage solution lose, on average, 17% of cellular Hb over the maximum FDA approved storage period of 42 days.[32]

An alternative approach to label-free characterization of RBCs using imaging technology has recently been reported. Using quantitative phase imaging, QPI, and treating each RBC as a lens, this approach allows multiple different types of anemia to be correlated to RBC parameters obtained with the QPI algorithms. Types of anemia include IRIDA, thalassemia, HS, etc. [33, 34]

In this current study, we further characterize and quantify the aging process of RBCs in storage by attempting to correlate this loss of Hb to the translocation of phosphatidylserine, PS, from the intracellular side of the RBC membrane to the extracellular side of the RBC membrane. We will also demonstrate that a significant number of microvesicles, expressing PS and containing a range of Hb concentrations, are associated with this ex vivo aging process, i.e., in the blood bank.

Experimental Methods

Sample Preparation

The method of obtaining and processing human RBC units has been previously reported and will only briefly be presented here.[33,34] Five expired, pre-storage leukoreduced human RBC units in AS-5 solution (composition presented in supplemental information) were obtained from a local FDA-licensed blood center. All blood samples were obtained using IRB approved protocols including informed consent. These units had been stored between 1 - 6 ºC for 42 days, the maximum FDA permitted storage shelf life. Expired RBC units were used for these experiments, since they would presumably have higher levels of PS expression compared to RBC units that had not been stored as long. The protocol for obtaining RBCs was approved by the University of Pittsburgh's institutional review board. The size distribution and concentration of RBCs was measured using a B23005 Multisizer 4e automated instrument (Beckman Coulter, CA). Osmolality of the various buffers were determined using an Osmoette A™ model 5002 Automatic Osmometer, (Precision Systems Inc., MA). As previously demonstrated, the metHb form of RBCs has nearly the exact same magnetic susceptibility compared to deoxygenated form of RBCs. Therefore, for ease of study, only the metHb form of Hb/RBCs were used. The metHb state of RBCs was created as previously reported in the literature.[30,32,34] Next, the metHb containing RBCs were stained with Annexin-V FLUOS (Roche, Switzerland) for 1 hour at room temperature in the dark and washed at 1000 g centrifugation with PBS.

Flow Cytometry

Met-RBCs, labeled with Annexin V-FLOUS, were sorted into four sub-populations based on the fluorescence intensity of the samples (high, medium, low and negative Annexin-V FLUOS expression) using a flow cytometer BD FACSARIA III (BD Biosciences, US). The sort was operated until 500,000 events were collected in each of the four sub-populations.

Cell Tracking Velocimetry

For the CTV instrument configuration reported in this study, the magnetic field parameters were S_m = 365 T*A/mm^2 ± 0.7%, and the mean field gradient was 0.755 T^2/mm over the field of view, FOV. The standard gravitational acceleration is g = 9.81 m/s^2, resulting in g/S_m = 2.68 × 10^{-8} m^3/kg. The volume magnetic susceptibility of the suspending fluid was taken as equal to that of water, χ_{fluid} = -9.035 × 10^{-6} (in SI system of units). The CTV software is capable of tracking on the order of thousands of cells, and for the experiments presented in this report, greater than 1,200 RBCs were tracked per experimental condition using the following procedure: the sorted metHb RBCs following the flow cytometric sorting were loaded into the CTV channel, (each fraction had approximately the same volume of 1 ml) and the channels were sealed on both ends (using valves) enabling the fluidic environment in the channel to reach steady state. After the samples began to settle, images of the settling RBCs were captured (50 video images in 1 s interval) and further processed using an in-house analysis program for calculation of the magnetic/settling velocity. Next, the analyzed samples were removed from the CTV instrument, and were subsequently characterized using the B23005 Multisizer 4e Coulter Counter, CC.

Statistical Analysis

To evaluate the reliability of the data obtained from the CTV system, the means and standard deviations (STD) of the ratio of induced velocities, u_m/u_s, from the particles in each sample, and the

repeated measures from the same sample, as well as the coefficient of variance (CV=STD/average ratio) for each sample were calculated. The changes of the ratios over time for each sample were estimated using the 2-sample t-test.

Results

A total of five, expired, human RBC units were investigated. Figure 1 presents the work flow of blood samples starting from the storage bag to final CC and CTV analysis. Figure 2 presents a set of representative images of a flow cytometry analysis and subsequent sorting. Figure 2A is a scatter plot of the forward/side scatter, while 2B and 2C present the "gating" analysis used for selection of "singlets" and removal of "duplets". Figure 2D presents the range of Annexin-V FLUOS expression (x-axis). The four sorted fractions were contained within the four boxes in this figure labeled P4 through P7.

Figure 3 presents a scatter plot, and corresponding histograms, of the settling velocity versus the magnetic velocity of the four sorted fractions based on PS expression. The most striking observations of these scatter plots is the dense concentration of PS negative events (black dots) and conversely, the much wider distribution of the events from the samples containing different levels of PS expression. The shaded region of the settling velocity values below 0.005 mm/s corresponds to velocity at which CV values begin to significantly increase.[31]

As has been presented in the equations above, and previous publications,[30,32] the mass of hemoglobin (pgHb/cell), and the diameter of the cell (or event) can be determined from these values of u_s and u_m. Figure 4 presents a scatter plot, 4A, and corresponding, relative frequency histograms, of the negative, and high PS expression sub-fraction "events" converted to diameter, in meters, and picograms of Hb per event. For the constants needed to convert the velocities into diameter and Hb concentration (Equations 2, 4-6) the previously published constants, and experimentally determined density were used.[34] Since, independently determined size measurements were made with a CC on the same samples immediately after CTV analysis, a histogram of the relative frequency of the measured diameters are included in this figure next to the calculated diameter histogram, Figure 4D.

Inspection of Figures 4C and 4D presents both information that confirms what was expected and surprising results. The similarity of the shape and the location of the peaks at approximately 4.8 microns for the PS negative cell populations (Figures 4C and 4D) 4D confirms that these peaks correspond to RBC(s) (PS negative cells). However, closer inspection indicates that the peaks with high PS expression, moves from the calculated diameter range of approximately 3.5 to 6 microns (Figure 4C), to 0.5 to 3 microns in 4D, thereby indicating that the cells that express the most PS externally are also some of the smallest cells measured. (Note, the aperture used in the CC analysis only allow particles greater than 0.5 microns and larger to be detected). Thus, as RBCs age and express PS, they also appear to shed membrane and become smaller in size.

To further highlight this size distribution, Figure 5 presents CC analysis of each sorted fraction, negative through high PS expression. Since the relative number of small cells/events significantly increased with increasing PS expression, an enlargement in the size range of 4 to 6 microns, and 0 to 2 microns is included to highlight the shift to smaller events as PS expression increased. To assist in further understanding the difference in event sizes, a control was also included which represents the CC electrolyte. For all samples analyzed, a dilution of 1:20 of sample to electrolyte was used. Since we are interested in these small events, the CC electrolyte was filtered using a 0.2 and 0.1 micron dead end filter. While Figure 5 presents the results for one of the stored RBC samples, the other four stored samples also demonstrated very similar results.

A common assumption with flow cytometry is that the forward scatter signal corresponds to the size of the event, and the side scatter signal corresponds to the granularity of the event, (the upper left scatter plot in Figure 2). Since BD FACSDIVA™ software was used in the sorting performed in this study, it is possible to determine the location of the specific dots for each of the sorted sub-fractions, P4 through P7. Given the gating strategy used, and highlighted in Figure 2, all of the events in P4 through P7 must be in the selected regions highlighted. Further, by color coding each of the events in P4-P7, it is possible to observe the specific location of these sub-fractions in the original scatter plot of side scatter vs forward scatter. For all five RBC samples tested, no discernible trends in the location in the side scatter vs forward scatter could be observed.

Inspection of Figure 5 indicates that the least number of events in the size range of a RBC is observed with the high expression PS events. Again, this observation was confirmed in all five of the stored RBC units. Equation 2 indicates that if the experimentally measured values of settling velocity and size can be made, the only adjustable variable is the density difference between the event and the suspending fluid. Assuming for all five RBC units and an average value of the diameter of these CC measured, PS expressing events to be 0.8 x 10^{-6} m, and an average settling velocity of 2 x 10^{-6} m/s, a density difference of approximately 5,623 kg/m^3 is obtained compared to the experimentally measured density difference of RBCs of 100 kg/m^3. With this average value of density, the mass of Hb per event can be subsequently calculated. Table 1 present a summary of this analysis of the five different stored RBC samples demonstrating a general similarity between samples.

A concern can be raised that the results presented above could be an artefact of changes in the osmolarity of the various suspending solutions used in this study. Table 2 presents the experimentally measured values, and the range of reported values in the human body. [35]

Discussion

In this study, three distinct instruments, two commercially available, and one unique to our laboratory, were used to characterize five RBC units that had expired, i.e, had been stored for >42 days. Each of these instruments allows distinct and complementary measurements of cells and smaller vesicles including: fluorescent signal, size, and magnetic susceptibility. This study was designed to build upon our previous study in which we demonstrated that RBCs lose, on average, 17% of their cellular Hb during the 42 day FDA approved storage period.[32]

Since PS expression on the surface of RBCs is a well-known marker of RBC aging, we used RBC surface PS expression to sort RBC into multiple sub-fractions with the intent of correlating the extent of PS expression with the cell's Hb content. While we were able to fractionate RBCs into four sub-fractions based on PS expression using a flow cytometer, the negative PS expressed sub-fraction was composed of predominately RBCs, while the sub-fractions with varying levels of PS expression, to our surprise, was mostly composed of smaller Hb containing microvesicles with significantly higher density than typical RBCs; It is this higher density which resulted in a settling velocity that is similar to actual RBCs with lower density (Figure 4C).

It is tempting to suggest that these smaller microvessicles are an artifact of the analysis process. While it is known, and quantitatively demonstrated that the hydrodynamics in a flow cytometer are sufficient to actually damage cells,[36] it is typically assumed that such damage would result in complete destruction of the cells with only cell debris present. Conversely, not only are we able to sort small vesicles that appear on the flow cytometer to be normal RBC expressing various levels of Annexin-V FLUOS but the concentration of Hb within the vesicles was orders of magnitude higher than typical RBCs. For example, Table 1 indicates that there was 3 to 5 pgHb/microvesicle, which is approximately 25% of the Hb content in a fully sized RBC with negative Annexin-V FLUOS expression, yet the volume of microvesicles was over 1/220th of a RBC. Pure disruption, i.e., membrane rupture and the ensuing destruction of the cell should not result in microvesicles with significantly higher concentration of Hb, as we report here. While the calculated density of these microvesicles might appear to be high, 5,623 kg/m^3, the high amount of Hb calculated per microvesicle, based on experimentally observed magnetophoretic mobility, suggests that these microvesicles are shrunken RBCs, consisting mostly of iron and protein.

These results, while only a "snapshot" of aged RBCs, present interesting questions for future studies. For example, are these magnetic microvesicles present in normal blood or is this observation an artifact of the ex vivo storage process? Is there a progression of microvesicles that form, and bleb off the RBCs as they age, or is this 1-micron vesicles just completely shrunken RBCs that have also lost some, but not all Hb/iron? The scatter plots in Figure 4 indicates that there are microvesicles that are still magnetic and those that are not. Is this the final state of the RBCs? Further, Annexin V negative RBCs had a mean Hb content of 21 pgHb/cell, below the generally accepted level for the diagnosis of anemia. While anemic, are these old RBCs still fully functional?

Table 2 indicates that the FDA storage buffer, AS-5, has an approximately 20 percent higher osmolality than human body fluids. At this time we do not know if this contributes to observations presented in this report, including the loss of haemoglobin.

Future studies will address these and related questions in blood in various stages of storage and we will investigate normal human blood to observe whether these 1 micron, PS expressing entities can be detected.

Conflicts of interest

There are no conflicts to declare.

Acknowledgements

We wish to thank the National Heart, Lung, and Blood Institute (1R01HL131720-01A1), DARPA (BAA07-21), and partial support from NIH (GRT00043657) for financial assistance.

All experimental procedures were performed in with approval of University of Pittsburg IRB, and blood samples were obtained using IRB approved protocols including informed consent.

References

1 K. D. Ellingson, M. R. P. Sapiano, K. A. Haass, A. A. Savinkina, M. L. Baker, K.-W. Chung, R. A. Henry, J. J. Berger, M. J. Kuehnert and S. V. Basavaraju, Transfusion, 2017, 57, 1588–1598.
2 M. H. Yazer, B. Jackson, N. Beckman, S. Chesneau, P. Bowler, M. Delaney, D. Devine, S. Field, M. Germain, M. F. Murphy, M. Sayers, B. Shaz, E. Shinar, M. Takanashi, R. Vassallo, C. Wickenden, V. Yahalom, K. Land and Biomedical Excellence for Safer Transfusions (BEST) Collaborative, Transfusion, 2016, 56, 1965–1973.
3 M. K. Fung, A. Eder, S. L. Spitalnik, C. M. Westhoff and AABB, Technical manual, .
4 N. Beckman, M. Yazer, K. Land, S. Chesneau and J. Caulfield, Transfus. Med., 2016, 26, 170–176.
5 S. M. Glasgow, S. Allard, H. Doughty, P. Spreadborough and E. Watkins, Transfus. Med., 2012, 22, 244–250.
6 K. K. S. Kuruppu, Biologicals, 2010, 38, 87–90.
7 A. Orbach, O. Zelig, S. Yedgar and G. Barshtein, Transfus. Med. Hemotherapy, 2017, 44, 183–187.
8 M. Luten, B. Roerdinkholder-Stoelwinder, N. P. M. Schaap, W. J. de Grip, H. J. Bos and G. J. C. G. M. Bosman, Transfusion, 2008, 48, 1478–1485.
9 A. TINMOUTH and I. CHINYEE, Transfus. Med. Rev., 2001, 15, 91–107.
10 M. J. Vandromme, G. McGwin and J. A. Weinberg, Scand. J. Trauma. Resusc. Emerg. Med., 2009, 17, 35.
11 A. B. Zimrin and J. R. Hess, Vox Sang., 2009, 96, 93–103.
12 C. G. Koch, P. I. Figueroa, L. Li, J. F. Sabik, T. Mihaljevic and E. H. Blackstone, Ann. Thorac. Surg., 2013, 96, 1894–1899.
13 J. Rawn, Curr. Opin. Anaesthesiol., 2008, 21, 664–668.
14 A. C. Zubair, Am. J. Hematol., 2009, 85, NA-NA.
15 L. van de Watering, Vox Sang., 2011, 100, 36–45.
16 M. I. Barnhart and J. M. Lusher, Am. J. Pediatr. Hematol. Oncol., 1979, 1, 311–30.
17 J. P. Atkinson, A. D. Schreiber and M. M. Frank, J. Clin. Invest., 1973, 52, 1509–1517.
18 R. E. Mebius and G. Kraal, Nat. Rev. Immunol., 2005, 5, 606–616.
19 F. A. Wagener, A. Eggert, O. C. Boerman, W. J. Oyen, A. Verhofstad, N. G. Abraham, G. Adema, Y. van Kooyk, T. de Witte and C. G. Figdor, Blood, 2001, 98, 1802–11.
20 D. J. Schaer and A. I. Alayash, Antioxid. Redox Signal., 2010, 12, 181–184.
21 R. P. Rother, L. Bell, P. Hillmen and M. T. Gladwin, JAMA, 2005, 293, 1653.
22 E. A. Hod, G. M. Brittenham, G. B. Billote, R. O. Francis, Y. Z. Ginzburg, J. E. Hendrickson, J. Jhang, J. Schwartz, S. Sharma, S. Sheth, A. N. Sireci, H. L. Stephens, B. A. Stotler, B. S. Wojczyk, J. C. Zimring and S. L. Spitalnik, Blood, 2011, 118, 6675–6682.
23 E. A. Hod, N. Zhang, S. A. Sokol, B. S. Wojczyk, R. O. Francis, D. Ansaldi, K. P. Francis, P. Della-Latta, S. Whittier, S. Sheth, J. E. Hendrickson, J. C. Zimring, G. M. Brittenham and S. L. Spitalnik, Blood, 2010, 115, 4284–4292.
24 C. Donadee, N. J. H. Raat, T. Kanias, J. Tejero, J. S. Lee, E. E. Kelley, X. Zhao, C. Liu, H. Reynolds, I. Azarov, S. Frizzell, E. M. Meyer, A. D. Donnenberg, L. Qu, D. Triulzi, D. B. Kim-Shapiro and M. T. Gladwin, Circulation, 2011, 124, 465–476.
25 C. D. Reiter, X. Wang, J. E. Tanus-Santos, N. Hogg, R. O. Cannon, A. N. Schechter and M. T. Gladwin, Nat. Med., 2002, 8, 1383–1389.
26 J. H. Baek, F. D'Agnillo, F. Vallelian, C. P. Pereira, M. C. Williams, Y. Jia, D. J. Schaer and P. W. Buehler, J. Clin. Invest., 2012, 122, 1444–1458.
27 L. Pauling and C. D. Coryell, Proc. Natl. Acad. Sci., 1936, 22, 210–216.
28 L. Pauling and C. D. Coryell, Repr. Erom Proc. NATIOPUL Ac~osaa~ Sci., 1936, 22, 159–163.
29 J. J. Chalmers, S. Haam, Y. Zhao, K. McCloskey, L. Moore, M. Zborowski and P. S. Williams, Biotechnol. Bioeng., 1999, 64, 519–26.
30 M. Zborowski, G. R. Ostera, L. R. Moore, S. Milliron, J. J. Chalmers and A. N. Schechter, Biophys. J., 2003, 84, 2638–45.
31 M. Nakamura, M. Zborowski, L. C. Lasky, S. Margel and J. J. Chalmers, Exp. Fluids, 2001, 30, 371–380.
32 J. J. Chalmers, X. Jin, A. F. Palmer, M. H. Yazer, L. Moore, P. Amaya, K. Park, X. Pan and M. Zborowski, Anal. Chem., 2017, 89, 3702–3709.
33 L. Miccio, P. Memmolo, F. Merola, P.A. Netti, P. Ferraro. Nature Communications. 2015,6:6502
34 M. Mugnano, P. Memmolo, L. Miccio, F. Merola, V. Bianco, A. Bramanti, A. Gabmbale, R. Russo, I. Andolfo, A. Iolascon, P. Farraro. Anal. Chem., 2018, 90, 7495-7501.
35. J. Xu, K. Mahajan, W. Xue, J. O. Winter, M. Zborowski and J. J. Chalmers, J. Magn. Magn. Mater., 2012, 324, 4189–4199.
34 X. Jin, M. H. Yazer, J. J. Chalmers and M. Zborowski, Analyst, 2011, 136, 2996.
35 A Comparative Study of Osmolarity Vs. Osmolality Vs. Tonicity, https://sciencestruck.com/osmolarity-vs-osmolality-vs-tonicity, (accessed November 27, 2018).
36. M. Mollet, R. Godoy-Silva, C. Berdugo and J. J. Chalmers, Biotechnol. Bioeng., 2008, 100, 260–272.

Figure Legends

Figure 1. Work flow for RBC analysis. RBCs were removed from the RBC unit and the number and size of RBCs characterized by the Multisizer 4e. Cells were oxidized to metHb RBCs and subsequently stained with Annexin-V FLUOS, and washed. This stained population was sorted into four sub-populations by flow cytometry based on Annexin-V FLUOS expression. Within several hours after sorting, the subfraction was characterized via CTV, cells collected, and analyzed with the Coulter Counter.

Figure 2 Representative flow cytometry analysis, including Annexin-V FLOUS expression level corresponding to the four sub-populations.

Figure 3. Scatter plot, and corresponding histograms, of the settling velocity and magnetic velocity for one of the five RBC units.

Figure 4. Scatter plot, 4A, and corresponding histograms, 4B and 4C, of the calculated RBC diameter, and amount of Hb per cell (pg Hb/cell) for the Annexin-V FLOUS negative and highest expressing subpopulations. A second histogram, 4D, of the experimentally measure diameters using the Coulter Counter is presented on the far right.

Figure 5. Histograms of the Coulter Counter analysis for each of the five sorted sub-populations. To assist in visualizing the results, enlargements in the 0 to 2 micron, and 4 to 6 microns size ranges are provided.

Table

Table 1. Summary of the RBC concentration in each of the five expired samples, as well and the average percent of the events that expressed no, low, medium, or high PS expression. For each of these four subpopulations, the average, calculated pgHb/event is presented.

		PS negative		**PS low**		**PS medium**		**PS high**	
sample	Cell conc. (Cells/ml)	% of events	pgHb/event	% of events	pgHb/event	% of events	pgHb/event	% of events	pgHb/event
A	1.20E+08	90	20.7 ±16	5	3.0	4	5.3	1	0.0
B	5.40E+07	90	17.9 ±6.7	6	3.8	3	3.8	1	1.9
C	1.00E+08	90	20.5 ±7.3	6	4.3	4	5.9	1	4.8
D	9.80E+07	86	21.9 ±6.4	6	4.0	6	3.4	2	3.3
E	8.60E+07	75	26.4 ±8.1	9	5.8	13	5.3	4	5.0
Mean	9.16E+07		21.5		4.2		4.7		3.0

Table 2. Osmolality of the various solutions used in this study, and the reported range of osmolality in human body fluids.

Solution	Osmolarity [mOsm/kg]
AS-5	370
PBS	300
FACS Sheath Fluid	348.5
Body fluid	270-300

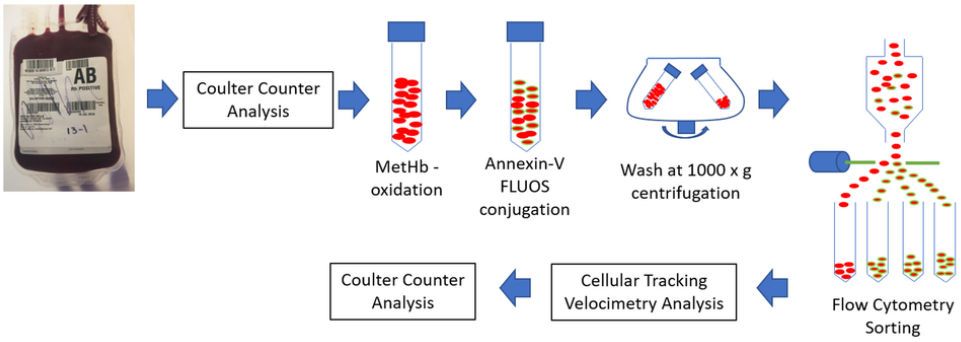

Figure 1

83x29mm (300 x 300 DPI)

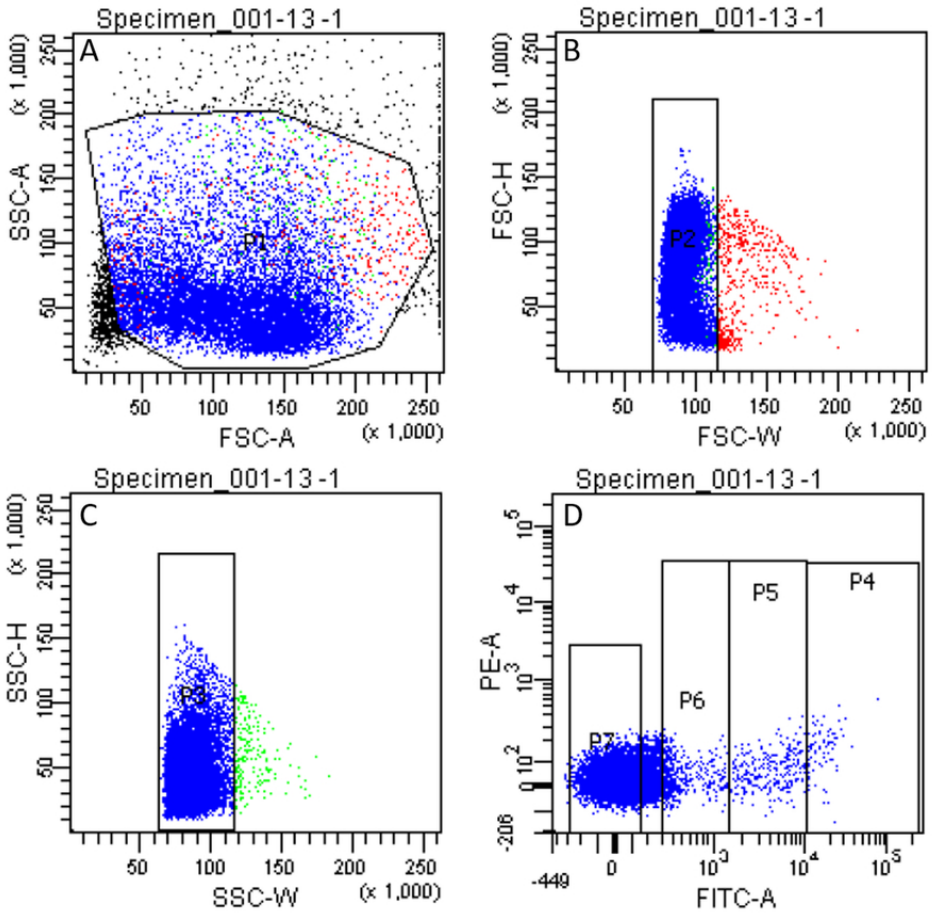

Figure 2

79x76mm (300 x 300 DPI)

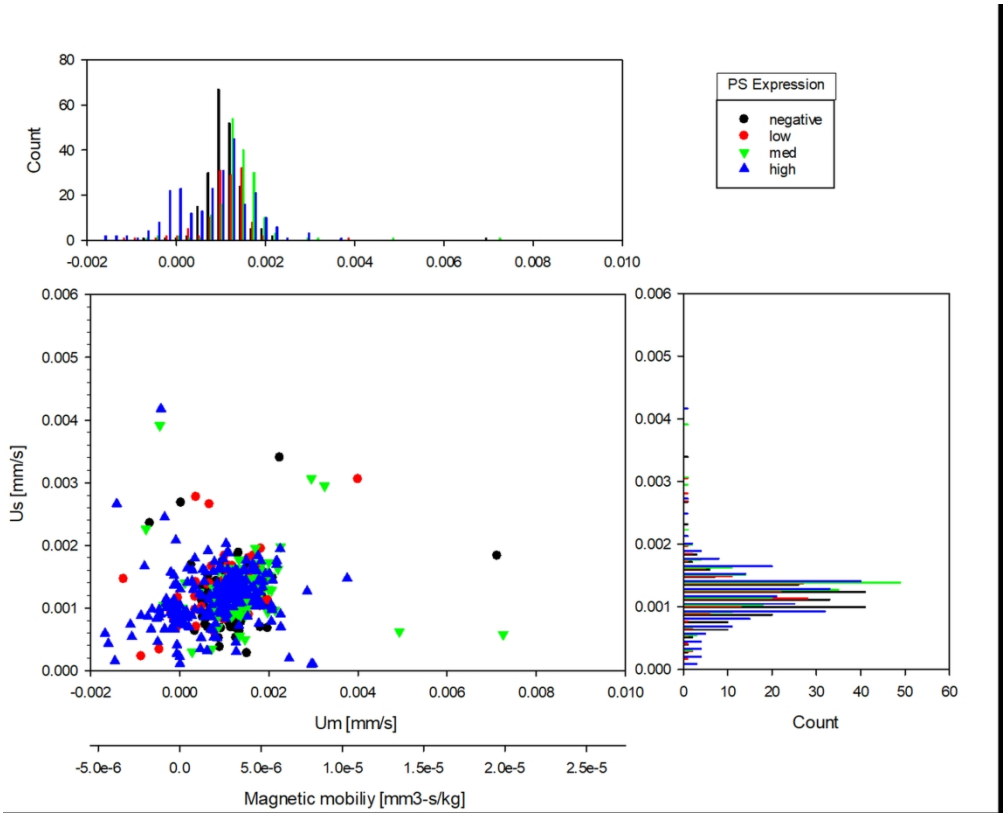

Figure 3

188x152mm (300 x 300 DPI)

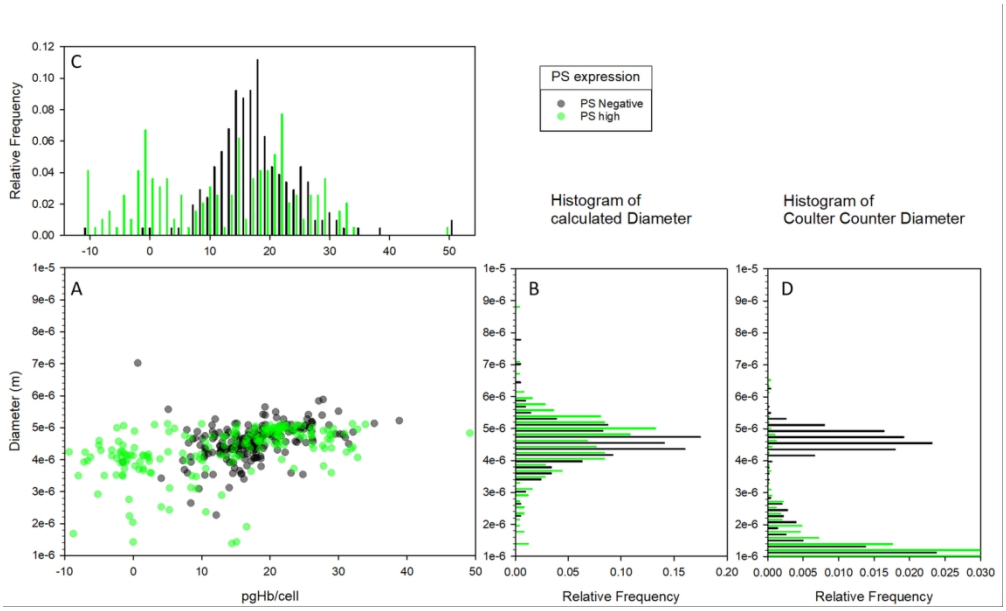

Figure 4

140x84mm (300 x 300 DPI)

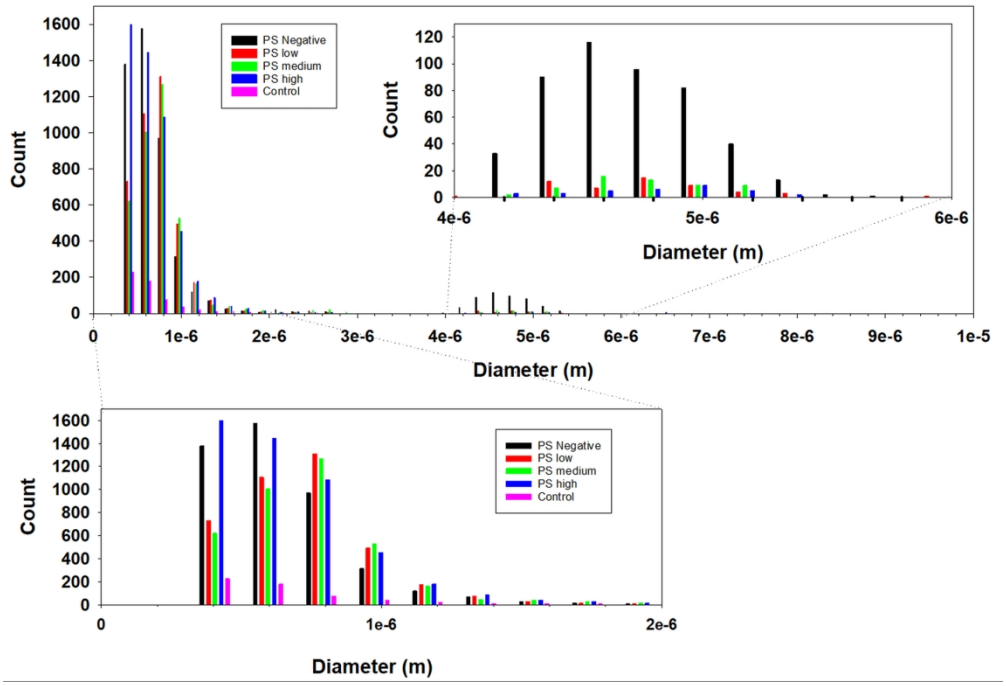

Figure 5

170x124mm (300 x 300 DPI)